https://doi.org/10.5194/acp-2020-1199
Preprint. Discussion started: 4 January 2021

Atmospheric Chemistry and Physics
Discussions
Open Access

Substantial changes of gaseous pollutants and chemical compositions in fine particles in North China Plain during COVID-19 lockdown period: anthropogenic vs meteorological influences

Rui Li[a], Yilong Zhao[a], Hongbo Fu[a, b] *

[a] *Shanghai Key Laboratory of Atmospheric Particle Pollution and Prevention, Department of Environmental Science & Engineering, Institute of Atmospheric Sciences, Fudan University, Shanghai, 200433, P.R. China*

[b] *Collaborative Innovation Center of Atmospheric Environment and Equipment Technology (CICAEET), Nanjing University of Information Science and Technology, Nanjing 210044, P.R. China*

*** Correspondence to:**

Prof. Fu (Email: fuhb@fudan.edu.cn)

Abstract

The rapid response to COVID-19 pandemic led to the unprecedented decreases of economic activities, thereby reducing the pollutant emissions. A random forest (RF) model was applied to determine the respective contributions of meteorology and anthropogenic emissions to the changes of air quality. The result suggested the strict lockdown measures significantly decreased primary components such as Cr (-201%) and Fe (-154%) in $PM_{2.5}$, whereas the higher relative humidity (RH) and NH_3 level, and the lower air temperature (T) enhanced the production of secondary aerosol including SO_4^{2-} (47.2%), NO_3^- (38.6%), and NH_4^+ (22.7%). Positive matrix factorization (PMF) result suggested that the contribution ratios of secondary formation (SF), industrial process (IP), biomass burning (BB), coal combustion (CC), and road dust (RD) changed from 35.2%, 28.9%, 19.4%, 11.8%, and 4.75% before COVID-19 outbreak to 42.7%, 20.5%, 19.45%, 9.80%, and 7.56%, respectively. The rapid increase of the contribution ratio derived from SF to $PM_{2.5}$ implied the

https://doi.org/10.5194/acp-2020-1199
Preprint. Discussion started: 4 January 2021

intermittent haze events during COVID-19 period were characterized with secondary aerosol pollution, which was mainly contributed by the unfavorable meteorological conditions and high NH_3 level.

1. Introduction

In December 2019, a cluster of pneumonia cases with unknown etiology were firstly reported in Wuhan and quickly spread around the world (Wu et al., 2020). The continuous global outbreak of coronavirus disease (COVID-19), declared as a public health emergency of international concern by the World Health Organization, resulted in unprecedented public health responses in many countries including lockdown, travel restrictions, and quarantines (Griffiths, J. and A. Woodyatt, 2020; Horowitz et al., 2020). On January 23, 2020, Chinese government imposed a lockdown in Wuhan and many surrounding cities in Hubei province in order to prevent the spread of epidemic. Afterwards, many similar measures including blocked roads, shutdown of factories, restricted citizen mobility, and checkpoints were soon extended to other cities throughout the entire country. During this period, energy production by coal-fired power plants only remained two thirds levels of the same periods in preceding years (Chang et al., 2020). Besides, the transport volume have been reduced by more than 70% due to the COVID-19 outbreak (Chang et al., 2020). These drastic government-enforced lockdown measures substantially decreased the pollutant emissions, and at least partly improved local air quality. Feng et al. (2020) confirmed that the COVID-19 lockdown have led to more than 70% reduction of NO_x emissions in many large cities over China. Correspondingly, the ambient $PM_{2.5}$ and NO_2 concentrations decreased by 35% and 60%, respectively (Shi and Brasseur, 2020). The natural experiment provided an unprecedented opportunity to explore the potential for emission reduction and the corresponding response of air

https://doi.org/10.5194/acp-2020-1199
Preprint. Discussion started: 4 January 2021

quality.

A growing body of studies assessed the response of $PM_{2.5}$ and gaseous pollutants to COVID-19 lockdown, and found these stringent restrictions resulted in the significant decreases of these pollutant (e.g., $PM_{2.5}$, NO_2, and CO) concentrations (Miyazaki et al., 2020; Marlia et al., 2020). However, some haze events still occurred during this period especially in East China. Huang et al. (2020) inferred these extraordinary findings might be attributable to enhanced secondary pollution based on the chemical transport models (CTMs). Understanding the formation mechanism of puzzle haze events depending on CTMs alone might be not very robust, it was highly imperative to perform more field observation to analyze the temporal variations of chemical compositions especially the secondary ions (e.g., SO_4^{2-}, NO_3^-) in $PM_{2.5}$ before and after COVID-19 outbreak and then to validate these inferences.

To date, only several field observations analyzed the temporal variations of chemical components in fine particles during COVID-19 lockdown period. Chang et al. (2020) observed a remarkably enhanced nitrate formation in Yangtze River Delta (YRD) neutralized the decreases of primary components in fine particles, which was in good agreement with the modelling result drawn by Huang et al. (2020). In contrast, Xu et al. (2020) found that the marked decreases of fine particles in Lanzhou during COVID-19 lockdown period was mainly contributed by the lower production rate for secondary aerosols. Under the condition of similar emission control measures, the polarized conclusion might be associated with the local meteorology. He et al. (2017) demonstrated that meteorology might explain more than 70% variances of daily average pollutant levels over China during 2014-2015. Besides, Zhang et al. (2020) also revealed that the higher relative humidity (RH) and the lower air temperature were beneficial to the secondary formation of primary emissions.

https://doi.org/10.5194/acp-2020-1199
Preprint. Discussion started: 4 January 2021

Thus, in order to accurately assess the effects of lockdown measures on air quality and to reveal the key driver of the haze paradox, it was necessary to isolate the contribution of meteorology. Unfortunately, up to date, the respective contributions of emission and meteorology to chemical compositions in $PM_{2.5}$ during COVID-19 period were not quantified yet in most pioneering studies (Chang et al., 2020; Huang et al., 2020; Xu et al., 2020). Moreover, the comparison of source contributions to chemical compositions between pre-lockdown and post-lockdown were scarcely performed. Such knowledge was critical to design effective $PM_{2.5}$ mitigation strategies in the near future.

As a heavily industrialized region, North China Plain (NCP) possesses many energy-intensive industries including coal-fired power plants, non-ferrous smelting industries, textiles, building materials, chemical engineering, and papermaking industries (Ren et al., 2011). Due to these intensive industrial emissions, NCP suffered from poor air quality and frequent aerosol pollution in the past decades (Zhang et al., 2018; Luo et al., 2017). Nevertheless, these strict lockdown measures during COVID-19 period inevitably led to the dramatic decreases of industrial emissions, and thus a study about the response of chemical compositions to emission reduction in the heavy-pollution city might make more sense.

Here, we selected the typical industrial city (Tangshan) in NCP to determine the concentrations of gaseous pollutants and chemical compositions in $PM_{2.5}$ during January 1-March 31, 2020, and then to analyze their temporal variations before and after COVID-19 outbreak. Besides, a machine-learning approach was applied to separate the contributions of emission reduction and meteorology to the temporal variabilities of chemical compositions and gaseous pollutants. Finally, the source apportionment was performed based on the meteorology-normalized datasets to compare the source difference for these pollutants before and after COVID-19 lockdown.

2. **Materials and methods**

2.1 Field observation

Hourly gaseous pollutants and $PM_{2.5}$ chemical compositions including water-soluble ions and trace elements were measured using on-line instruments during January 1-March 31, 2020 at a supersite in Tangshan. The supersite is located in a commercial region without short-distance industrial emissions (Figure 1). SO_2, NO_2, and CO concentrations were determined by the ultraviolet fluorescence analyzer (TEI, Model 43i from Thermo Fisher Scientific Inc., USA), chemiluminescence trace gas analyzer (TEI Model 42i from Thermo Fisher Scientific Inc., USA), and the correlation infrared absorption analyzer (TAPI, model: 300E, USA) (Li et al., 2017; Li et al., 2019). The $PM_{2.5}$ concentration was determined using an oscillating balance analyzer (TH-2000Z, China) (Wang et al., 2014). The NH_3 concentration and water-soluble ions including sulfate (SO_4^{2-}), nitrate (NO_3^-), ammonium (NH_4^+), sodium ion (Na^+), and chloridion (Cl^-) were monitored with a Gas and Aerosol Collector combined with Ion Chromatography (GAC-IC, TH-PKU-303, China) (Wang et al., 2014; Zheng et al., 2019). Nine trace elements including Hg, Pb, K, Ca, Cr, Cu, Fe, Ni, and Zn were determined by an online multi-element analyzer (Model Xact 625, Cooper Environment Service, USA). The quality assurance of SO_2, NO_2, CO, and $PM_{2.5}$ were conducted based on HJ 630-2011 specifications. For the quality assurance of NH_3 and water-soluble ions, the concentration gradients of anion and cation standard solutions were set based on the pollution levels of target species, and correlation coefficients of the calibration curve must be higher than 0.999. Besides, a standard sample was collected each day and the relative standard deviation for the reproducibility test must be less than 5%. The online device agreed well with the result determined

https://doi.org/10.5194/acp-2020-1199
Preprint. Discussion started: 4 January 2021

Atmospheric Chemistry and Physics Discussions

by filter sampling coupled with Inductively Coupled Plasma Mass Spectrometry (ICP-MS) and Inductively Coupled Plasma-Atomic Emission Spectroscopy (ICP-AES).

2.2 Deweathered model development

The air pollutants were influenced by the combined effects of meteorological conditions and emissions. In order to quantify the contributions of anthropogenic emissions, the impacts of meteorological conditions should be removed. In our study, a random forest (RF) approach was employed to serve as the site-specific modeling platform. All of gaseous pollutants and chemical compositions in $PM_{2.5}$ were regarded as the dependent variables. The meteorological parameters (WS, WD, T, RH, Prec, and P), and time predictors (year, DOY, DOW, hour) served as the independent variables. The original dataset was randomly classified into a training dataset (90% of input dataset) for developing the RF model and the remained one was treated as the test dataset. After the building of the RF model, the deweathered technique was applied to predict the air pollutant level at a specific time point (e.g., 2020/01/01 12:00). The differences of original pollutant concentrations and deweathered pollutant concentrations were regarded as the concentrations contributed by meteorology.

2.3 Source apportionment

Positive matrix factorization (PMF 5.0) model version was used to perform the $PM_{2.5}$ source apportionment. The deweathered gaseous pollutants and chemical compositions in $PM_{2.5}$ were input into the model. The objective of PMF is to resolve the issues of chemical mass balance between measured concentration of each species and its source contributions by decomposing the input matrix into factor contribution and factor profile. The detailed equation is shown in Eq. (1)-(2). Briefly, the basic principle of PMF is to calculate the least object function Q when the g_{ik} must be a

https://doi.org/10.5194/acp-2020-1199
Preprint. Discussion started: 4 January 2021

positive-definite matrix based on Eq. (2) (Chen et al., 2014; Sharma et al., 2016).

$$x_{ij} = \sum_{k=1}^{p} g_{ik} f_{kj} + e_{ij} \quad (1)$$

$$Q = \sum_{i=1}^{n} \sum_{j=1}^{m} [\frac{x_{ij} - \sum_{k=1}^{p} g_{ik} f_{kj}}{u_{ij}}]^2 \quad (2)$$

where x_{ij} and e_{ij} represent the concentration and uncertainty of jth species, respectively. g_{ik} represents the contribution ratio of kth source to ith sample, f_{kj} represents the ratio of jth species in kth source, and e_{ij} indicates the residual of jth species in the i sample. The uncertainties associated with factor profiles were evaluated using three error calculation methods including bootstraps (BS) method, displacement (DISP) analysis, and the combination method of DISP and BS (BS-DISP). For the BS method, 100 runs were performed and the result has been believed to be valid since all of the factors showed a mapping of above 90%. DISP analysis also confirmed that the solution was considered to be stable because the observed drop in the Q value was less than 0.1% and no factor swap occurred. For the BS-DISP analysis, the solution has been verified to be useful because the observed drop in the Q value was less than 0.5%. Furthermore, both of the results from BS and BS-DISP did not suggest any asymmetry or rotational ambiguity for all of the factors (Manousakas et al., Brown et al., 2015).

3. **Results and discussion**

3.1 The concentration changes of gaseous pollutants and $PM_{2.5}$ chemical compositions

Figure 2-4 show the temporal variations of gaseous pollutants and chemical compositions in $PM_{2.5}$ from January 1-March 31, which could be divided into two periods including before and after COVID-19 outbreak. In this study, January 23 was regarded as the breakpoint because China's government imposed a lockdown in Wuhan and surrounding cities. Before COVID-19 outbreak, the

https://doi.org/10.5194/acp-2020-1199
Preprint. Discussion started: 4 January 2021

average observed concentrations of SO_2, NO_2, CO, and NH_3 during January 1-22 were 34.4 μg/m^3, 63.5 μg/m^3, 1.97 mg/m^3, and 13.6 ppb, respectively. After COVID-19 lockdown, the mean concentrations of these gaseous pollutants changed to 25.3 μg/m^3, 39.0 μg/m^3, 1.62 mg/m^3, and 18.3 ppb, respectively. Overall, SO_2, NO_2, and CO concentrations decreased by 36.3%, 62.8%, and 21.3%, respectively, whereas the NH_3 concentration increased by 25.8%.

As shown in Figure 2, the chemical compositions in $PM_{2.5}$ also showed dramatic changes during January 1-March 31 due to the impact of COVID-19 lockdown. The observed $PM_{2.5}$, SO_4^{2-}, Na^+, and Cl^- concentrations decreased by 15.3%, 6.67%, 93.5%, and 40.8%, respectively, while observed NO_3^- (2.17%) and NH_4^+ (7.02%) levels showed slight increases. In Shanghai, Chen et al. (2020) revealed that SO_4^{2-}, and NH_4^+ concentrations displayed significant decreases after COVID-19 outbreak due to the obvious decreases of precursor concentrations (e.g., SO_2, NO_x). However, both of observed NO_3^- and NH_4^+ concentrations in Tangshan even showed slight increases though the NO_2 concentration suffered remarkable decrease. It was assumed that the adverse meteorological conditions might be beneficial to the pollutant accumulation (Zheng et al., 2019; Zhang et al., 2019b). Besides, the concentrations of nine trace elements were also determined. The observed values of Pb (68.8%), Ca (64.2%), Cr (69.2%), Cu (7.44%), Fe (32.6%), and Zn (91.5%) suffered from dramatic decreases, while the Hg (20.0%), K (0.08%), and Ni (1.17%) concentrations still displayed stable increases. As a whole, the temporal variability of these elements in Tangshan before and after COVID-19 lockdown was in agreement with the result in Beijing (He et al., 2017). However, the K concentration in Beijing showed rapid decrease after COVID-19 outbreak, which was not in coincident with our study (He et al., 2017). It suggested that the slight increase of K in Tangshan might be linked with the unfavorable meteorological conditions (He et al., 2017).

https://doi.org/10.5194/acp-2020-1199
Preprint. Discussion started: 4 January 2021

Atmospheric Chemistry and Physics Discussions

3.2 The impact of emission reduction on air quality

Although the observed concentrations of air pollutants can be applied to analyze the impact of COVID-19 lockdown, the role of emission reduction on air quality might be not clearly revealed because the meteorological factors were also important variables influencing the air pollutant concentrations. In order to accurately reflect the response of air quality to emission reduction during COVID-19 lockdown period, the meteorological conditions were isolated by machine-learning model. In our study, we developed a random forest model to remove the impacts of meteorological conditions on air pollutant. As shown in Figure S1-S3, the observed values showed the better correlation with the normalized values for most of the pollutants, indicating that the developed model was robust to remove the impact of meteorological conditions. The deweathered concentrations of gaseous pollutants and chemical compositions in $PM_{2.5}$ are depicted in Figure 2-4. The deweathered SO_2, NO_2, CO, and NH_3 concentrations decreased by 45.0%, 73.7%, 47.9%, and 30.9%, respectively during COVID-19 lockdown period compared with before COVID-19 outbreak. Meanwhile, the normalized-meteorology $PM_{2.5}$, SO_4^{2-}, NO_3^-, NH_4^+, Na^+, and Cl^- concentrations decreased by 61.7%, 53.9%, 36.4%, 15.7%, 87.9%, and 54.6%, respectively. For trace elements, deweathered Pb, K, Ca, Cr, Cu, Fe, Ni, and Zn levels reduced by 146%, 29.0%, 118%, 201%, 18.2%, 155%, 37.1%, and 219%, respectively. Nevertheless, the deweathered Hg concentration still kept stable increase by the rate of 18.0% compared with the period before COVID-19 outbreak.

As shown in Figure 2-4, the deweathered concentrations for most of the pollutants showed significant decreases after COVID-19 outbreak compared with the period before COVID-19. It was assumed that many cities proposed the lockdown measures, which significantly minimized

https://doi.org/10.5194/acp-2020-1199
Preprint. Discussion started: 4 January 2021

industrial, transportation, and commercial activities. Among all of the pollutants, the deweathered Zn, Cr, Fe, Pb, Ca, NH_4^+, $PM_{2.5}$, NO_2, SO_4^{2-}, and Na^+ experienced more than 50% decrease rates due to the lockdown measures. It was well known that Zn, Cr, and Fe originated mainly from metallurgical industry (Sun et al., 2018; Zhu et al., 2018), while Pb might be derived from coal-fired power plants (Cui et al., 2019; Meng et al., 2020). During the COVID-19 outbreak, most of the industries have been shut down and energy production by coal-fired power plants was reduced by one third (Chang et al., 2020). Thus, these element concentrations suffered from dramatic decreases. It should be noted that the deweathered Ca concentration also decreased by more than 100%. It was well documented that the Ca was often associated with the dust resuspension (Chang et al., 2018). In fact, the Ca was known as one of the most abundant elements in the upper continental crust, which was likely originated from the road fugitive dust (Chang et al., 2018; Shen et al., 2016). More than 70% reduction of vehicle transportation and domestic flights facilitated the rapid decrease of Ca concentration (Chang et al., 2020). Besides, $PM_{2.5}$ and some water-soluble ions including deweathered SO_4^{2-} and NH_4^+ concentrations also experienced marked decreases after COVID-19 lockdown, which was in good agreement with their gaseous precursors. It might be attributable to the rapid decreases of precursor emissions. The deweathered Na^+ concentration showed the rapid decrease after COVID-19 lockdown, which suggested that the Na^+ in the $PM_{2.5}$ of Tangshan was probably derived from waste incineration rather than sea-salt aerosol (Deshmukh et al., 2016).

Although most of pollutant concentrations suffered remarkable decreases, the decrease ratios of deweathered NH_3 and NH_4^+ concentrations after COVID-19 outbreak were far lower than those of many other gaseous pollutants and water-soluble ions. It was attributable to the fact that the contributions of fossil fuel and urban waste sources increased after COVID-19 outbreak (Zhang et al., 2020b). Besides, it should be noted that the normalized-meteorology Hg concentration still remained the stable increase. It was supposed that the Hg was mainly released from the coal combustion for domestic heating (Zhou et al., 2018), which was not restricted during the COVID-19 lockdown period.

3.3 The role of meteorology on air quality

Compared with the observed values, the deweathered concentrations of most pollutants were significantly reduced. Meanwhile, the deweathered decrease ratios of pollutants were significantly higher than those of observed values. The result suggested the meteorology conditions during the COVID-19 lockdown period were not favorable to the pollutant dispersion, as evidenced by some recent studies (Chang et al., 2020; Huang et al., 2020).

As shown in Figure 5, the contributions of meteorological conditions to pollutants remained to be positive, and their contributions to water-soluble ions and NH_3 concentrations were remarkably higher than those to other gaseous pollutants and trace elements, suggesting that these chemical compositions more sensitive to meteorological variations. In our study, six meteorological parameters including WS, WD, T, RH, Prec, and P have been integrated into the random forest model to assess the response of each species to different meteorological variables. The variable importance suggested that the mass concentrations of most species were sensitive to RH (Figure 6-8). Both of T and WD were key factors for trace elements, while T and P were responsible for the variability of water-soluble ions. Deshmukh et al. (2016) confirmed that the high RH promoted the aqueous-phase oxidation of SO_2 and the production of sulfate. Tian et al. (2019) also demonstrated that RH-dependent heterogeneous reactions significantly contributed to the sulfate generation and the high RH enhanced gas- to aqueous-phase dissolution of NH_3 and HNO_3. These pioneering experiments suggested that secondary aerosols were often formed under the condition of high RH. Very recently, Chang et al. (2020) observed that the nitrate concentration in YRD experienced unusual increase during COVID-19 period, while Xu et al. (2020) obtained the opposite result in Lanzhou. It was assumed that the persistent increase of T and decrease of RH in Lanzhou during this period was not beneficial to the generation of secondary aerosol, while the high RH in YRD significantly elevated local nitrate level. Compared with the water-soluble ions, some trace elements such as Fe and Zn on the mineral/soot surface only catalyzed the heterogeneous generation of sulfate and nitrate, which was less sensitive to RH than water-soluble ions (Hu et al., 2015). Except RH, the trace elements were mainly affected by both of T and WD. The higher temperature often resulted in the lower water content in the soil and a higher tendency of dust suspension (Lyu et al., 2016). As shown in Figure 8, the Ca concentration was significantly influenced by T because Ca was mainly enriched in the fugitive dust. The trace element concentrations were also affected by WD. It was assumed that the strong northwestern winds during the dust events led to higher concentrations of Ca and Fe concentrations. In addition, the neighboring industrial points including cement plants and coal-fired power plants also affected the concentrations of trace elements via long/short-range transport, which was strongly dependent on WD.

Unlike the trace elements, water-soluble ions were frequently affected by T and P rather than WD. Wu et al. have found that the heterogeneous oxidation of SO_2 by ozone was sensitive to the variation of T, and showed a turning point for sulfate formation rate around 250 K (Wu et al., 2011). Major water-soluble ions in $PM_{2.5}$ including SO_4^{2-}, NO_3^-, and NH_4^+ were mainly derived from secondary formation rather than the direct emission (Feng et al., 2020a; Zhang et al., 2020a), and thus they were not very sensitive to WD.

https://doi.org/10.5194/acp-2020-1199
Preprint. Discussion started: 4 January 2021

3.4 The enhanced secondary aerosol formation during COVID-19 lockdown period

The deweathered chemical compositions suggested that the sulfate and nitrate chemistry changed slightly after COVID-19 outbreak. The oxidation ratio of sulfate (SOR, the ratio of sulfate concentration and the sum of sulfate and SO_2 concentrations) decreased from 0.26 to 0.22, while the oxidation ratio of nitrate (NOR, the ratio of nitrate concentration and the sum of nitrate and NO_2 concentrations) increased from 0.22 to 0.25 (Table 1). The decreased SOR after COVID-19 outbreak indicated that the decrease rate of sulfate is higher than that of SO_2. In contrast, the increased NOR during COVID-19 lockdown period revealed that the decrease rate of nitrate is lower than that of NO_2. The increased NOR after COVID-19 outbreak suggested the consecutive nitrate production, though the NO_2 emission experienced tremendous reduction, which was in good agreement with the result observed by Chang et al. (2020). It was assumed that the persistently higher observed NH_3 concentration during this period promoted the ammonium nitrate formation though the lower NO_x emission (Zhang et al., 2020b), which also partially explained the abnormal increases of observed concentrations of secondary ions after COVID-19 outbreak. In general, NH_3 firstly tends to react with H_2SO_4 to form ammonium sulfate, and then the excess NH_3 participated in the reaction with HNO_3 (Chen et al., 2019; Zhang et al., 2019a). However, sulfate concentration suffered from more dramatic decrease compared with SO_2, which might be associated with the aerosol acidity during COVID-19 lockdown period. The ratio of NH_4^+ and the sum of SO_4^{2-}, NO_3^-, and Cl^- named C/A was regarded as an indicator to reflect the aerosol acidity. In our study, the C/A value decreased from 0.33 to 0.28 after COVID-19 outbreak, implicating that the aerosol acidity even showed slight increase during the COVID-19 lockdown period. It was well known that the higher aerosol acidity might prohibit the conversion from SO_2 to sulfate (Liu et al., 2020; Shao et al., 2019), which yielded

https://doi.org/10.5194/acp-2020-1199
Preprint. Discussion started: 4 January 2021

the lower SOR.

3.5 The impact of COVID-19 lockdown on source apportionment

The emission control measures inevitably triggered the variation of source apportionment (Liu et al., 2017; Meng et al., 2020). In the present study, Positive matrix factorization (PMF 5.0) was employed to identify the major sources of $PM_{2.5}$ in Tangshan before and after COVID-19 outbreak. About 3-9 factor solutions were examined, and a five-factor solution obtained the lowest Q (robust) and Q (true) values. Additionally, the PMF analysis and error diagnostics also suggested the result was robust (Table S1-S3).

The source apportionment profiles in pre-COVID and post-COVID resolved by PMF are depicted in Figure 9. For pre-COVID, the first factor contributed 35.2% to the total species. The factor was characterized with high levels of NH_4^+ (41.1%), SO_4^{2-} (35.8%), and NO_3^- (33.9%). SO_4^{2-} and NO_3^- were generally produced by oxidation of SO_2 and NO_x, respectively. The NH_4^+ was often formed through the heterogeneous reaction of NH_3 and sulfate or HNO_3. Thus, the factor was regarded as the secondary formation (SF). The second factor was characterized with high loadings of Zn (48.7%), Cr (43.1%), Fe (42.3%), and Pb (30.1%). Cr and Fe were mainly originated from fuel combustion and metallurgical industry such as chrome plating and steel production(Liu et al., 2018a), while Pb and Zn was derived from the roasting, sintering and smelting process for the extraction of Pb/Zn ores (Wu et al., 2012). Therefore, the factor 2 was treated as the industrial process (IP) source. The predominant species in factor 3 included Na^+ (41.3%) and K (40.2%). K was often regarded as the fingerprint of biomass burning (BB) (Chen et al., 2017; Zheng et al., 2019b), whereas the Na^+ was generally regarded as the tracer of waste incineration (Alam et al., 2019; Durlak et al., 1997). Hence, the factor 3 was treated as the BB source. Tangshan suffered from

https://doi.org/10.5194/acp-2020-1199
Preprint. Discussion started: 4 January 2021

remarkable increasing usage of biomass fuels for domestic heating in winter, which promoted the emissions of K and Na^+ (Chen et al., 2017). The most abundant species in factor 4 were Hg (73.6%), Pb (69.4%), K (38.2%), Cu (34.2%), Cl^- (35.4%), and SO_4^{2-} (26.6%). Pb, Hg, and Cu were typical marker elements for coal combustion, and around 56% of Pb and 47% of Hg were released from coal combustion (Cheng et al., 2015; Zhu et al., 2020). In northern China, the coal-based domestic heating was one of the most important sector of coal consumption (Liu et al., 2018b). Dai et al. (2019) also verified that the residential coal combustion was major source of primary sulfate. Thus, the factor 4 was regarded as the coal combustion (CC) source. The last factor was distinguished by high loadings of Fe (47.0%), Ni (46.0%), and Ca (38.1%). Fe, Ni, and Ca were enriched in the brake wear and tyre wear dusts (Dehghani et al., 2017; Urrutia-Goyes et al., 2018), and thus the elements in this factor were mainly sourced from traffic-related road dust (RD).

After COVID-19 outbreak, the chemical compositions in $PM_{2.5}$ were also classified into five sources including SF, IP, BB, CC, and RD. However, the contribution ratios of these sources varied greatly after the implementation of serious lockdown measures. The contribution ratio of IP experienced the largest decrease from 28.9% to 20.5%, whereas the apportionment of SF showed the marked increase from 35.2% to 42.7%. The contributions of other three sources only suffered from slight variations. The rapid decrease of IP contribution might be associated with the shutdown of many industries during COVID-19 period (Zheng et al., 2020), while the obvious increase of SF contribution was attributable to more heterogeneous or aqueous reactions of precursors (Chang et al., 2020). For nearly all of the species, the contribution ratios of IP suffered from remarkable decreases after COVID-19 outbreak. The contribution ratios of SF for SO_4^{2-}, NO_3^-, and NH_4^+ increased from 35.8%, 33.9%, and 41.1% to 48.4%, 45.6%, and 49.9% after COVID-19 outbreak,

https://doi.org/10.5194/acp-2020-1199
Preprint. Discussion started: 4 January 2021

respectively. However, the contribution ratios of SF for other species remained relatively stable. It was assumed that SO_4^{2-}, NO_3^-, and NH_4^+ were mainly produced from secondary formation of precursors (Jiang et al., 2019; Yao et al., 2020), while other species especially the trace elements were mainly derived from the primary emission (Wu et al., 2020b). Although the COVID-19 pandemic led to the shutdown of many coal-fired power plants and industries and decreased the CC emissions from these sectors (Kraemer et al., 2020), the government-enforced home order might increase the electricity consumption (Venter et al., 2020), which offset the decreases of CC contributions to industrial activities. Therefore, the contribution ratios of CC did not experience dramatic variation after COVID-19 outbreak.

4. Conclusions and implications

The lockdown measures led to the shutdown of many industries, in turn resulting in the significant decreases of primary components in $PM_{2.5}$. We employed RF model to determine the respective contributions of meteorology and emission reduction on the variations of gaseous pollutants and $PM_{2.5}$ chemical compositions during COVID-19 lockdown period. The deweathered levels of some trace elements (e.g., Pb (-147%), Zn (-219%)) and water-soluble ions (e.g., SO_4^{2-} (-53.9%)) derived from industrial emissions experienced more than 50% decrease rates due to the stringent lockdown measures. However, the higher relative humidity (RH) and lower air temperature (T) significantly prohibited the decreases of water-soluble ion concentrations because they were beneficial to the heterogeneous or aqueous reaction of sulfate and nitrate. Trace elements were very sensitive to wind direction (WD) due to the long-range transport of anthropogenic emissions. Besides, the contributions of secondary formation to $PM_{2.5}$ increased from 35.2% to 42.7% after COVID-19 outbreak. The finding also explained that the opposite change trends of the secondary aerosols in East and West China found by previous studies was not only attributable to the large difference in meteorological conditions, but also the discrepancy of NH_3 concentration.

In the future work, it is necessary to seek multi-pollutants (e.g., VOC, NO_x) emission control measures to reduce the concentrations of primary and secondary components simultaneously since adverse meteorological conditions coupled with slightly higher oxidation capability especially in winter still caused the haze formation. Our results also highlight that more NH_3 emission control measures are urgently needed because the excess NH_3 could exacerbate the generation of secondary aerosols. Besides, the generation of primary pollutants was very sensitive to RH and WD. Thus, the primary pollutant emissions from the industries in the upwind direction should be strictly restricted.

Acknowledgements

This work was supported by National Natural Science Foundation of China (Nos. 91744205, 21777025, 21577022, 21177026), and Chinese Postdoctoral Science Foundation (2020M680589).

Author contributions

Hongbo Fu designed the study. Rui Li wrote the manuscript. Yilong Zhao analyzed the data.

Competing interests

The authors declare that they have no conflict of interest.

Data availability

The meteorological data are available in http://data.cma.cn/.

https://doi.org/10.5194/acp-2020-1199
Preprint. Discussion started: 4 January 2021

Atmospheric Chemistry and Physics
Discussions

Figure 1 The topographic map of China indicating the location of Tangshan (a), sampling site (b), and some key industrial points (b). The population density of Tangshan is also depicted in (b).

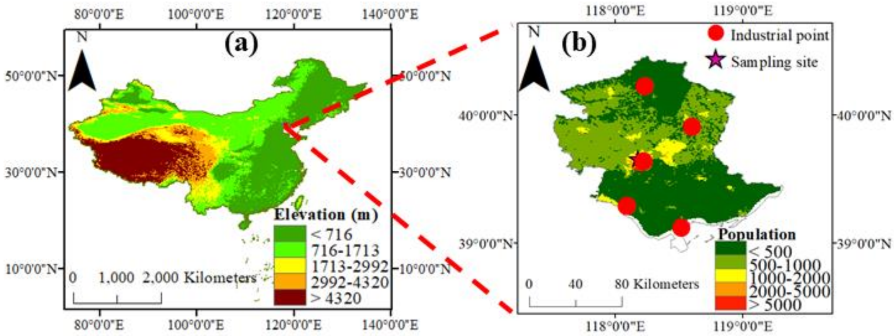

https://doi.org/10.5194/acp-2020-1199
Preprint. Discussion started: 4 January 2021

Figure 2 Observed and deweathered weekly concentrations and changes of gaseous pollutants during January 1st-March 31th. The black dotted line represent the date of COVID-19 lockdown in China. The white background denotes the changes of gaseous pollutants before COVID-19, while the faint yellow one represents the chemical components after COVID-19 outbreak.

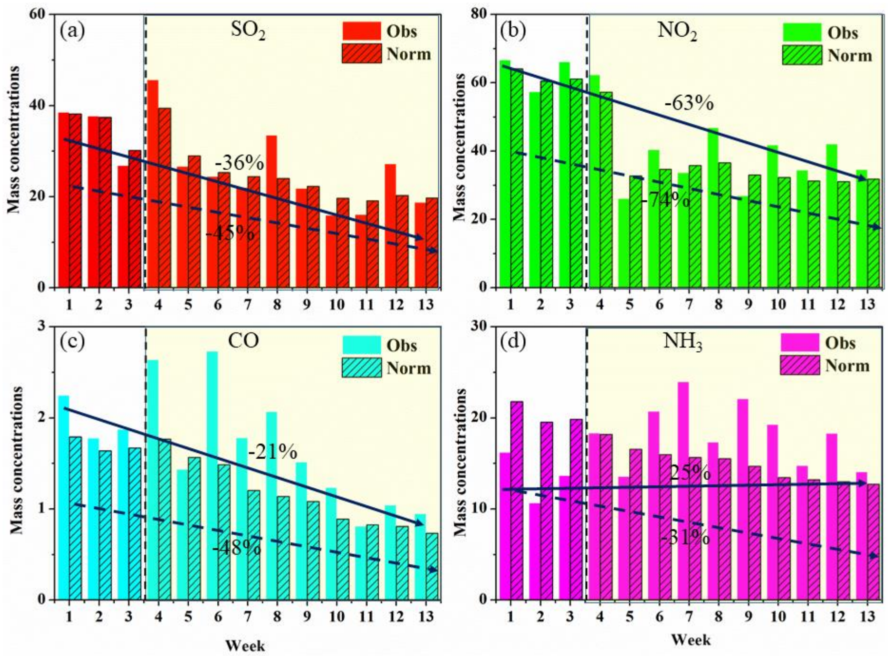

https://doi.org/10.5194/acp-2020-1199
Preprint. Discussion started: 4 January 2021

Atmospheric Chemistry and Physics
Discussions

Figure 3 Observed and deweathered weekly concentrations and changes of $PM_{2.5}$ and water-soluble ions during January 1st-March 31th. The black dotted line represent the date of COVID-19 lockdown in China. The white background denotes the changes of $PM_{2.5}$ and water-soluble ions before COVID-19, while the faint yellow one represents the chemical components after COVID-19 outbreak.

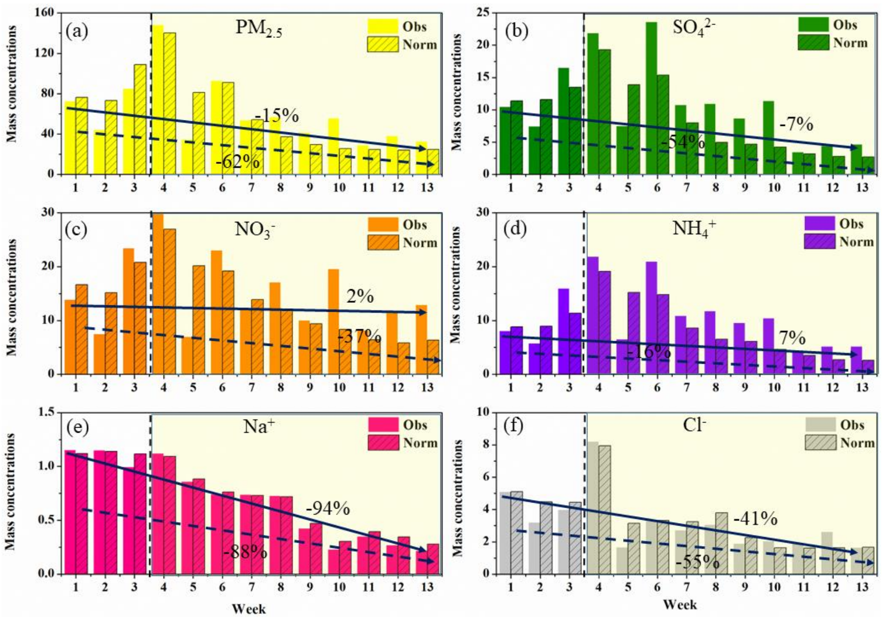

https://doi.org/10.5194/acp-2020-1199
Preprint. Discussion started: 4 January 2021

Atmospheric Chemistry and Physics
Discussions

Figure 4 Observed and deweathered weekly concentrations and changes of trace elements during January 1st-March 31th. The black dotted line represent the date of COVID-19 lockdown in China. The white background denotes the changes of trace elements before COVID-19, while the faint yellow one represents the chemical components after COVID-19 outbreak.

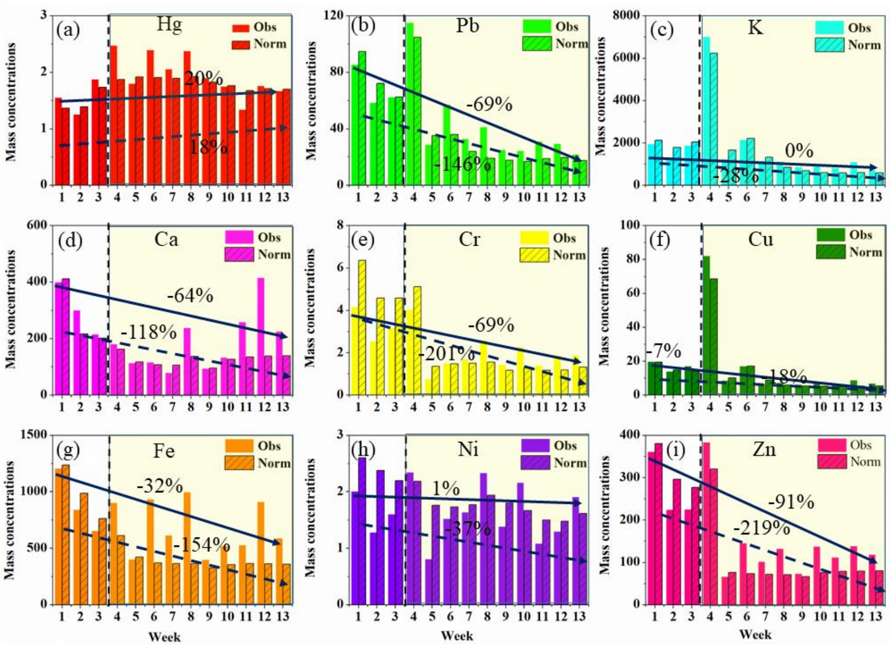

https://doi.org/10.5194/acp-2020-1199
Preprint. Discussion started: 4 January 2021

Figure 5 The changes of observed concentrations of multiple components between pre-lockdown and post-lockdown against the changes derived from the emission and meteorological changes.

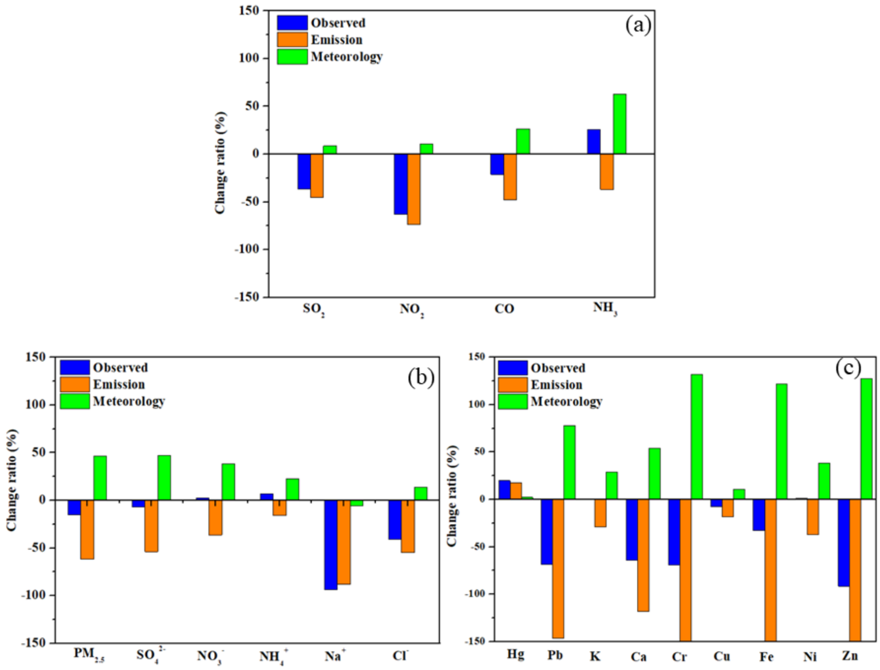

https://doi.org/10.5194/acp-2020-1199
Preprint. Discussion started: 4 January 2021

Figure 6 Relative importance of the predictors for the prediction of gaseous pollutants.

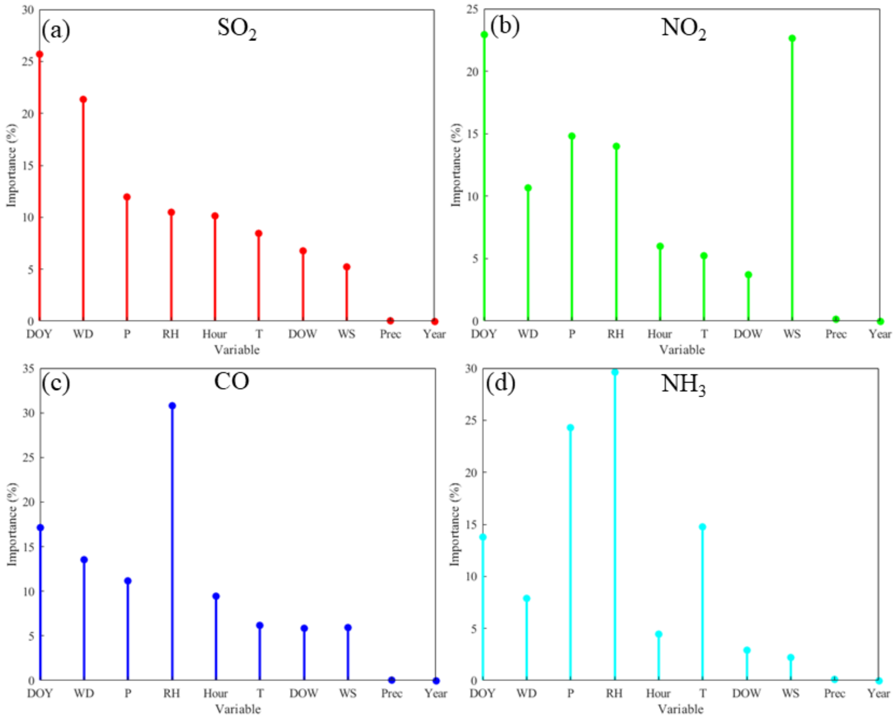

https://doi.org/10.5194/acp-2020-1199
Preprint. Discussion started: 4 January 2021

Atmospheric Chemistry and Physics
Open Access
Discussions

Figure 7 Relative importance of the predictors for the prediction of water-soluble ions in $PM_{2.5}$.

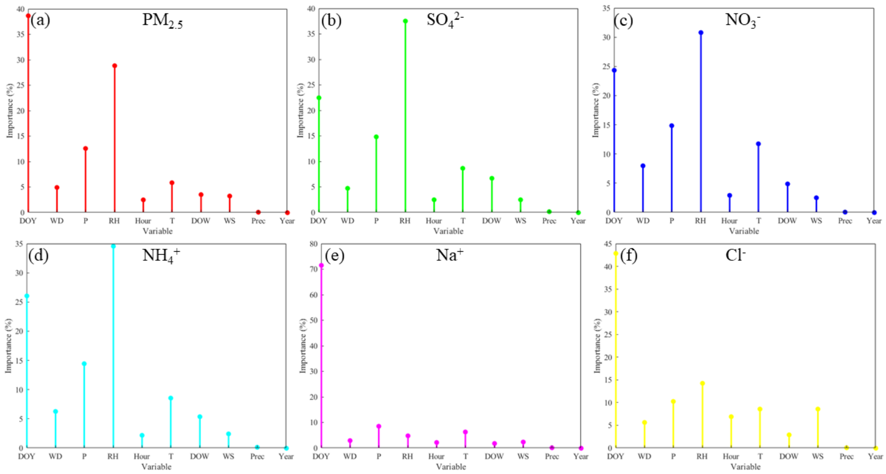

https://doi.org/10.5194/acp-2020-1199
Preprint. Discussion started: 4 January 2021

Atmospheric Chemistry and Physics
Open Access
Discussions

Figure 8 Relative importance of the predictors for the prediction of trace elements in $PM_{2.5}$.

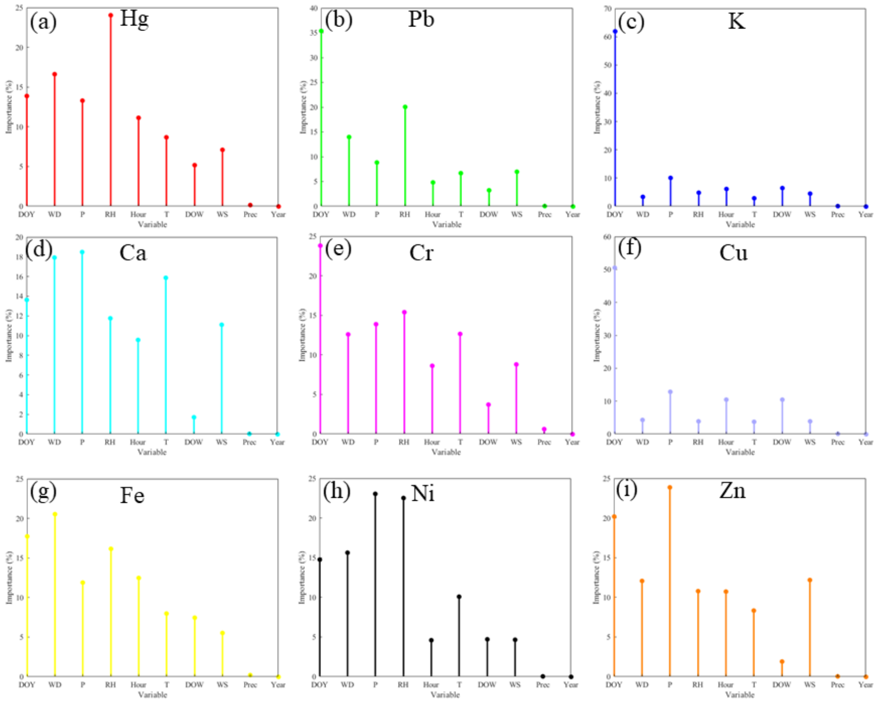

https://doi.org/10.5194/acp-2020-1199
Preprint. Discussion started: 4 January 2021

Atmospheric Chemistry and Physics Discussions
Open Access
EGU

Figure 9 The comparison of source apportionment for $PM_{2.5}$ chemical compositions before (a) and after (b) COVID-19 outbreak.

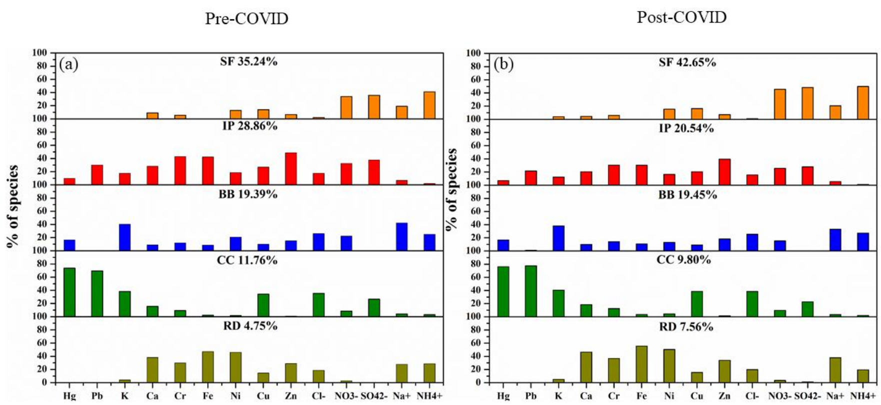

https://doi.org/10.5194/acp-2020-1199
Preprint. Discussion started: 4 January 2021

Table 1 SOR, NOR, and C/A values in Pre-COVID and Post-COVID (SOR = $SO_4^{2-}/(SO_4^{2-}+SO_2)$, NOR=$NO_3^-/(NO_3^-+NO_2)$, C/A=$NH_4^+/(SO_4^{2-}+NO_3^-+Cl^-)$).

	SOR	NOR	C/A
Pre-COVID	0.26	0.22	0.33
Post-COVID	0.22	0.25	0.28

https://doi.org/10.5194/acp-2020-1199
Preprint. Discussion started: 4 January 2021

References

Alam, Q., Hendrix, Y., Thijs, L., Lazaro, A., Schollbach, K., Brouwers, H., 2019. Novel low temperature synthesis of sodium silicate and ordered mesoporous silica from incineration bottom ash. Journal of Cleaner Production 211, 874-883.

Brown, S.G., Eberly, S., Paatero, P., Norris, G.A., 2015. Methods for estimating uncertainty in PMF solutions: Examples with ambient air and water quality data and guidance on reporting PMF results. Science of the Total Environment 518, 626-635.

Chang, Y., Huang, K., Xie, M., Deng, C., Zou, Z., Liu, S., Zhang, Y., 2018. First long-term and near real-time measurement of trace elements in China's urban atmosphere: temporal variability, source apportionment and precipitation effect. Atmos. Chem. Phys 18, 11793-11812.

Chang, Y., Huang, R.J., Ge, X., Huang, X., Hu, J., Duan, Y., Zou, Z., Liu, X., Lehmann, M.F., 2020. Puzzling haze events in China during the coronavirus (COVID-19) shutdown. Geophysical Research Letters 47, e2020GL088533.

Chen, H., Huo, J., Fu, Q., Duan, Y., Xiao, H., Chen, J., 2020. Impact of quarantine measures on chemical compositions of PM2. 5 during the COVID-19 epidemic in Shanghai, China. Science of The Total Environment 743, 140758.

Chen, J., Li, C., Ristovski, Z., Milic, A., Gu, Y., Islam, M.S., Wang, S., Hao, J., Zhang, H., He, C., 2017. A review of biomass burning: Emissions and impacts on air quality, health and climate in China. Science of the Total Environment 579, 1000-1034.

Chen, L., Gao, Y., Zhang, M., Fu, J.S., Zhu, J., Liao, H., Li, J., Huang, K., Ge, B., Wang, X., 2019. MICS-Asia III: Multi-model comparison and evaluation of aerosol over East Asia. Atmospheric Chemistry and Physics 19, 11911-11937.

Chen, W., Shao, M., Lu, S., Wang, M., Zeng, L., Yuan, B., Liu, Y., 2014. Understanding primary and secondary sources of ambient carbonyl compounds in Beijing using the PMF model. Atmospheric Chemistry & Physics 14.

Cheng, K., Wang, Y., Tian, H., Gao, X., Zhang, Y., Wu, X., Zhu, C., Gao, J., 2015. Atmospheric emission characteristics and control policies of five precedent-controlled toxic heavy metals from anthropogenic sources in China. Environmental science & technology 49, 1206-1214.

Cui, Y., Ji, D., Chen, H., Gao, M., Maenhaut, W., He, J., Wang, Y., 2019. Characteristics and sources of hourly trace elements in airborne fine particles in urban Beijing, China. Journal of Geophysical Research: Atmospheres 124, 11595-11613.

Cui, Y., Ji, D., Maenhaut, W., Gao, W., Zhang, R., Wang, Y., 2020. Levels and sources of hourly PM2. 5-related elements during the control period of the COVID-19 pandemic at a rural site between Beijing and Tianjin. Science of the Total Environment 744, 140840.

Dai, Q., Bi, X., Song, W., Li, T., Liu, B., Ding, J., Xu, J., Song, C., Yang, N., Schulze, B.C., 2019. Residential coal combustion as a source of primary sulfate in Xi'an, China. Atmospheric Environment 196, 66-76.

Dehghani, S., Moore, F., Keshavarzi, B., Beverley, A.H., 2017. Health risk implications of potentially toxic metals in street dust and surface soil of Tehran, Iran. Ecotoxicology and environmental safety 136, 92-103.

Deshmukh, D.K., Kawamura, K., Deb, M.K., 2016. Dicarboxylic acids, ω-oxocarboxylic acids, α-dicarbonyls, WSOC, OC, EC, and inorganic ions in wintertime size-segregated aerosols from central India: Sources and formation processes. Chemosphere 161, 27-42.

https://doi.org/10.5194/acp-2020-1199
Preprint. Discussion started: 4 January 2021

Durlak, S.K., Biswas, P., Shi, J., 1997. Equilibrium analysis of the affect of temperature, moisture and sodium content on heavy metal emissions from municipal solid waste incinerators. Journal of Hazardous Materials 56, 1-20.

Feng, J., Chan, E., Vet, R., 2020a. Air quality in the eastern United States and Eastern Canada for 1990–2015: 25 years of change in response to emission reductions of SO2 and NOx in the region. Atmospheric Chemistry & Physics 20.

Feng, S., Jiang, F., Wang, H., Wang, H., Ju, W., Shen, Y., Zheng, Y., Wu, Z., Ding, A., 2020b. NOx emission changes over China during the COVID-19 epidemic inferred from surface NO2 observations. Geophysical Research Letters, e2020GL090080.

Griffiths, J., Woodyatt, A., 2020. Wuhan coronavirus: Thousands of cases confirmed as China goes into emergency mode. CNN. Archived from the original on 28.

He, J., Gong, S., Yu, Y., Yu, L., Wu, L., Mao, H., Song, C., Zhao, S., Liu, H., Li, X., 2017. Air pollution characteristics and their relation to meteorological conditions during 2014–2015 in major Chinese cities. Environmental pollution 223, 484-496.

Horowitz, J., 2020. Italy locks down much of the country's north over the coronavirus. The New York Times. Available at https://www. nytimes. com/2020/03/07/world/europe/coronavirus-italy. html.

Hu, Y., Lin, J., Zhang, S., Kong, L., Fu, H., Chen, J., 2015. Identification of the typical metal particles among haze, fog, and clear episodes in the Beijing atmosphere. Science of the Total Environment 511, 369-380.

Huang, X., Ding, A., Gao, J., Zheng, B., Zhou, D., Qi, X., Tang, R., Wang, J., Ren, C., Nie, W., 2020. Enhanced secondary pollution offset reduction of primary emissions during COVID-19 lockdown in China. National Science Review.

Jiang, F., Liu, F., Lin, Q., Fu, Y., Yang, Y., Peng, L., Lian, X., Zhang, G., Bi, X., Wang, X., 2019. Characteristics and formation mechanisms of sulfate and nitrate in size-segregated atmospheric particles from urban Guangzhou, China. Aerosol and Air Quality Research 19, 1284-1293.

Kraemer, M.U., Yang, C.-H., Gutierrez, B., Wu, C.-H., Klein, B., Pigott, D.M., Du Plessis, L., Faria, N.R., Li, R., Hanage, W.P., 2020. The effect of human mobility and control measures on the COVID-19 epidemic in China. Science 368, 493-497.

Li, R., Cui, L., Li, J., Zhao, A., Fu, H., Wu, Y., Zhang, L., Kong, L., Chen, J., 2017. Spatial and temporal variation of particulate matter and gaseous pollutants in China during 2014–2016. Atmospheric Environment 161, 235-246.

Liu, B., Wu, J., Zhang, J., Wang, L., Yang, J., Liang, D., Dai, Q., Bi, X., Feng, Y., Zhang, Y., 2017. Characterization and source apportionment of PM2. 5 based on error estimation from EPA PMF 5.0 model at a medium city in China. Environmental Pollution 222, 10-22.

Liu, J., Chen, Y., Chao, S., Cao, H., Zhang, A., Yang, Y., 2018a. Emission control priority of PM2. 5-bound heavy metals in different seasons: A comprehensive analysis from health risk perspective. Science of the total environment 644, 20-30.

Liu, K., Wang, S., Wu, Q., Wang, L., Ma, Q., Zhang, L., Li, G., Tian, H., Duan, L., Hao, J., 2018b. A highly resolved mercury emission inventory of Chinese coal-fired power plants. Environmental science & technology 52, 2400-2408.

Liu, P., Ye, C., Xue, C., Zhang, C., Mu, Y., Sun, X., 2020. Formation mechanisms of atmospheric nitrate and sulfate during the winter haze pollution periods in Beijing: gas-phase, heterogeneous and aqueous-phase chemistry. Atmospheric Chemistry & Physics 20.

Luo, R., Han, Y., Liu, Z., 2017. The current status and factors of indoor PM2. 5 in Tangshan, China. Procedia Engineering 205, 3824-3829.

Lyu, X., Chen, N., Guo, H., Zeng, L., Zhang, W., Shen, F., Quan, J., Wang, N., 2016. Chemical characteristics and causes of airborne particulate pollution in warm seasons in Wuhan, central China. Atmospheric chemistry and physics.

Manousakas, M., Papaefthymiou, H., Diapouli, E., Migliori, A., Karydas, A., Bogdanovic-Radovic, I., Eleftheriadis, K., 2017. Assessment of PM2. 5 sources and their corresponding level of uncertainty in a coastal urban area using EPA PMF 5.0 enhanced diagnostics. Science of the Total Environment 574, 155-164.

Marlier, M.E., Xing, J., Zhu, Y., Wang, S., 2020. Impacts of COVID-19 response actions on air quality in China. Environmental Research Communications 2, 075003.

Meng, Y., Li, R., Zhao, Y., Cheng, H., Fu, H., Yan, Z., Bing, H., 2020. Chemical characterization and sources of PM2. 5 at a high-alpine ecosystem in the Southeast Tibetan Plateau, China. Atmospheric Environment, 117645.

Miyazaki, K., Bowman, K., Sekiya, T., Jiang, Z., Chen, X., Eskes, H., Ru, M., Zhang, Y., Shindell, D., 2020. Air Quality Response in China Linked to the 2019 Novel Coronavirus (COVID-19) Lockdown. Geophysical Research Letters 47, e2020GL089252.

Ren, Z., Zhang, B., Lu, P., Li, C., Gao, L., Zheng, M., 2011. Characteristics of air pollution by polychlorinated dibenzo-p-dioxins and dibenzofurans in the typical industrial areas of Tangshan City, China. Journal of Environmental Sciences 23, 228-235.

Shao, J., Chen, Q., Wang, Y., Lu, X., He, P., Sun, Y., Shah, V., Martin, R.V., Philip, S., Song, S., 2019. Heterogeneous sulfate aerosol formation mechanisms during wintertime Chinese haze events: air quality model assessment using observations of sulfate oxygen isotopes in Beijing. Atmospheric Chemistry and Physics 19.

Sharma, S., Mandal, T., Jain, S., Sharma, A., Saxena, M., 2016. Source apportionment of PM 2.5 in Delhi, India using PMF model. Bulletin of environmental contamination and toxicology 97, 286-293.

Shen, Z., Sun, J., Cao, J., Zhang, L., Zhang, Q., Lei, Y., Gao, J., Huang, R.-J., Liu, S., Huang, Y., 2016. Chemical profiles of urban fugitive dust PM2. 5 samples in Northern Chinese cities. Science of the Total Environment 569, 619-626.

Shi, X., Brasseur, G.P., 2020. The Response in Air Quality to the Reduction of Chinese Economic Activities during the COVID-19 Outbreak. Geophysical Research Letters, e2020GL088070.

Sun, W., Shao, M., Granier, C., Liu, Y., Ye, C., Zheng, J., 2018. Long-term trends of anthropogenic SO2, NOx, CO, and NMVOCs emissions in China. Earth's Future 6, 1112-1133.

Tian, M., Liu, Y., Yang, F., Zhang, L., Peng, C., Chen, Y., Shi, G., Wang, H., Luo, B., Jiang, C., 2019. Increasing importance of nitrate formation for heavy aerosol pollution in two megacities in Sichuan Basin, southwest China. Environmental Pollution 250, 898-905.

Urrutia-Goyes, R., Hernandez, N., Carrillo-Gamboa, O., Nigam, K., Ornelas-Soto, N., 2018. Street dust from a heavily-populated and industrialized city: Evaluation of spatial distribution, origins, pollution, ecological risks and human health repercussions. Ecotoxicology and environmental safety 159, 198-204.

Venter, Z.S., Aunan, K., Chowdhury, S., Lelieveld, J., 2020. COVID-19 lockdowns cause global air pollution declines with implications for public health risk. medRxiv.

Wang, Y., Ying, Q., Hu, J., Zhang, H., 2014. Spatial and temporal variations of six criteria air pollutants in 31 provincial capital cities in China during 2013-2014. Environment International 73, 413-

https://doi.org/10.5194/acp-2020-1199
Preprint. Discussion started: 4 January 2021

422.

Wu, F., Zhao, S., Yu, B., Chen, Y.-M., Wang, W., Song, Z.-G., Hu, Y., Tao, Z.-W., Tian, J.-H., Pei, Y.-Y., 2020a. A new coronavirus associated with human respiratory disease in China. Nature 579, 265-269.

Wu, L., Tong, S., Wang, W., Ge, M., 2011. Effects of temperature on the heterogeneous oxidation of sulfur dioxide by ozone on calcium carbonate. Atmospheric Chemistry & Physics Discussions 11.

Wu, Q., Wang, S., Zhang, L., Song, J., Yang, H., Meng, Y., 2012. Update of mercury emissions from China's primary zinc, lead and copper smelters, 2000-2010. Atmospheric Chemistry & Physics Discussions 12.

Wu, Y., Lin, S., Tian, H., Zhang, K., Wang, Y., Sun, B., Liu, X., Liu, K., Xue, Y., Hao, J., 2020b. A quantitative assessment of atmospheric emissions and spatial distribution of trace elements from natural sources in China. Environmental Pollution 259, 113918.

Xu, J., Ge, X., Zhang, X., Zhao, W., Zhang, R., Zhang, Y., 2020. COVID-19 impact on the concentration and composition of submicron particulate matter in a typical city of Northwest China. Geophysical Research Letters, e2020GL089035.

Xu, Q., Wang, S., Jiang, J., Bhattarai, N., Li, X., Chang, X., Qiu, X., Zheng, M., Hua, Y., Hao, J., 2019. Nitrate dominates the chemical composition of PM2.5 during haze event in Beijing, China. Science of The Total Environment 689, 1293-1303.

Yao, L., Wang, D., Fu, Q., Qiao, L., Wang, H., Li, L., Sun, W., Li, Q., Wang, L., Yang, X., 2019. The effects of firework regulation on air quality and public health during the Chinese Spring Festival from 2013 to 2017 in a Chinese megacity. Environment international 126, 96-106.

Yao, Q., Liu, Z., Han, S., Cai, Z., Liu, J., Hao, T., Liu, J., Huang, X., Wang, Y., 2020. Seasonal variation and secondary formation of size-segregated aerosol water-soluble inorganic ions in a coast megacity of North China Plain. Environmental science and pollution research international.

Zhang, K., Ma, Y., Xin, J., Liu, Z., Ma, Y., Gao, D., Wu, J., Zhang, W., Wang, Y., Shen, P., 2018. The aerosol optical properties and PM2. 5 components over the world's largest industrial zone in Tangshan, North China. Atmospheric Research 201, 226-234.

Zhang, Q., Zheng, Y., Tong, D., Shao, M., Wang, S., Zhang, Y., Xu, X., Wang, J., He, H., Liu, W., 2019a. Drivers of improved PM2. 5 air quality in China from 2013 to 2017. Proceedings of the National Academy of Sciences 116, 24463-24469.

Zhang, X., Murakami, T., Wang, J., Aikawa, M., 2020a. Sources, species and secondary formation of atmospheric aerosols and gaseous precursors in the suburb of Kitakyushu, Japan. Science of The Total Environment, 143001.

Zhang, Y., Liu, X., Fang, Y., Liu, D., Tang, A., Collett, J.L., 2020b. Atmospheric Ammonia in Beijing during the COVID-19 Outbreak: Concentrations, Sources, and Implications. Environmental Science & Technology Letters.

Zhang, Y., Vu, T.V., Sun, J., He, J., Shen, X., Lin, W., Zhang, X., Zhong, J., Gao, W., Wang, Y., 2019b. Significant Changes in Chemistry of Fine Particles in Wintertime Beijing from 2007 to 2017: Impact of Clean Air Actions. Environmental Science & Technology 54, 1344-1352.

Zheng, H., Kong, S., Chen, N., Yan, Y., Liu, D., Zhu, B., Xu, K., Cao, W., Ding, Q., Lan, B., 2020. Significant changes in the chemical compositions and sources of PM2. 5 in Wuhan since the city lockdown as COVID-19. Science of The Total Environment, 140000.

Zheng, H., Kong, S., Yan, Q., Wu, F., Cheng, Y., Zheng, S., Wu, J., Yang, G., Zheng, M., Tang, L., 2019a.

The impacts of pollution control measures on PM2.5 reduction: Insights of chemical composition, source variation and health risk. Atmospheric Environment 197, 103-117.

Zheng, H., Kong, S., Yan, Q., Wu, F., Cheng, Y., Zheng, S., Wu, J., Yang, G., Zheng, M., Tang, L., 2019b. The impacts of pollution control measures on PM2. 5 reduction: Insights of chemical composition, source variation and health risk. Atmospheric Environment 197, 103-117.

Zhou, S., Davy, P.K., Huang, M., Duan, J., Wang, X., Fan, Q., Chang, M., Liu, Y., Chen, W., Xie, S., 2018. High-resolution sampling and analysis of ambient particulate matter in the Pearl River Delta region of southern China: source apportionment and health risk implications. Atmospheric Chemistry and Physics 18, 2049-2064.

Zhu, C., Tian, H., Hao, J., 2020. Global anthropogenic atmospheric emission inventory of twelve typical hazardous trace elements, 1995–2012. Atmospheric Environment 220, 117061.

Zhu, C., Tian, H., Hao, Y., Gao, J., Hao, J., Wang, Y., Hua, S., Wang, K., Liu, H., 2018. A high-resolution emission inventory of anthropogenic trace elements in Beijing-Tianjin-Hebei (BTH) region of China. Atmospheric environment 191, 452-462.